Supporting Information

$Ni_3Se_4/Fe(PO_3)_2$/NF Composites as high-efficiency electrocatalysts with a low overpotential for the oxygen evolution reaction

Ting-Yu Shuai, Qi-Ni Zhan, Hui-Min Xu, Chen-Jin Huang, Zhi-Jie Zhang, Hong-Rui Zhu, Gao-Ren Li*

College of Materials Science and Engineering, Sichuan University, Chengdu 610065, China

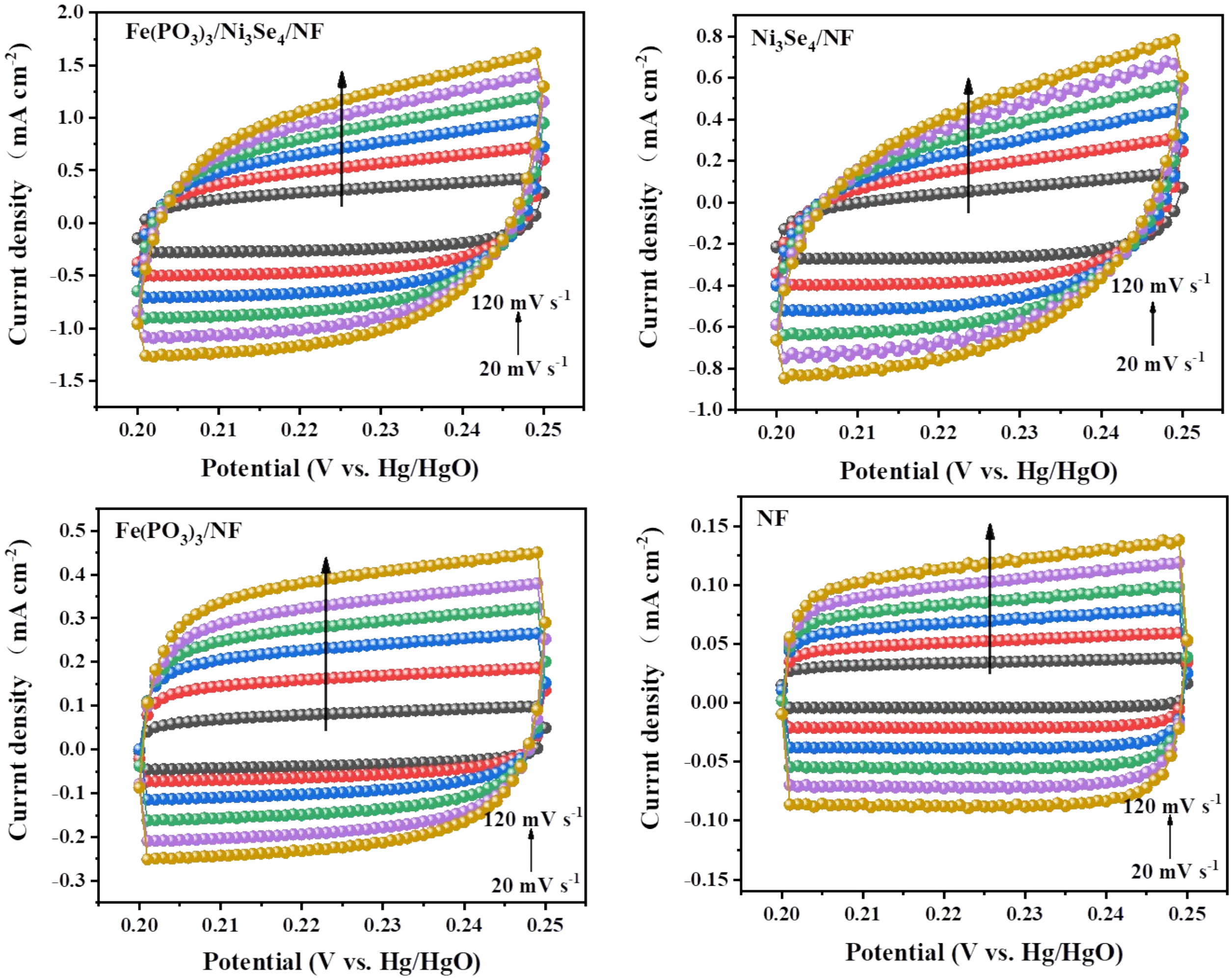

Fig. S1 CVs of (a) $Ni_3Se_4/Fe(PO_3)_2$/NF, (b)Ni_3Se_4/NF, (c) $Fe(PO_3)_2$/NF, (d) NF from 20 to 120 mV S^{-1}.

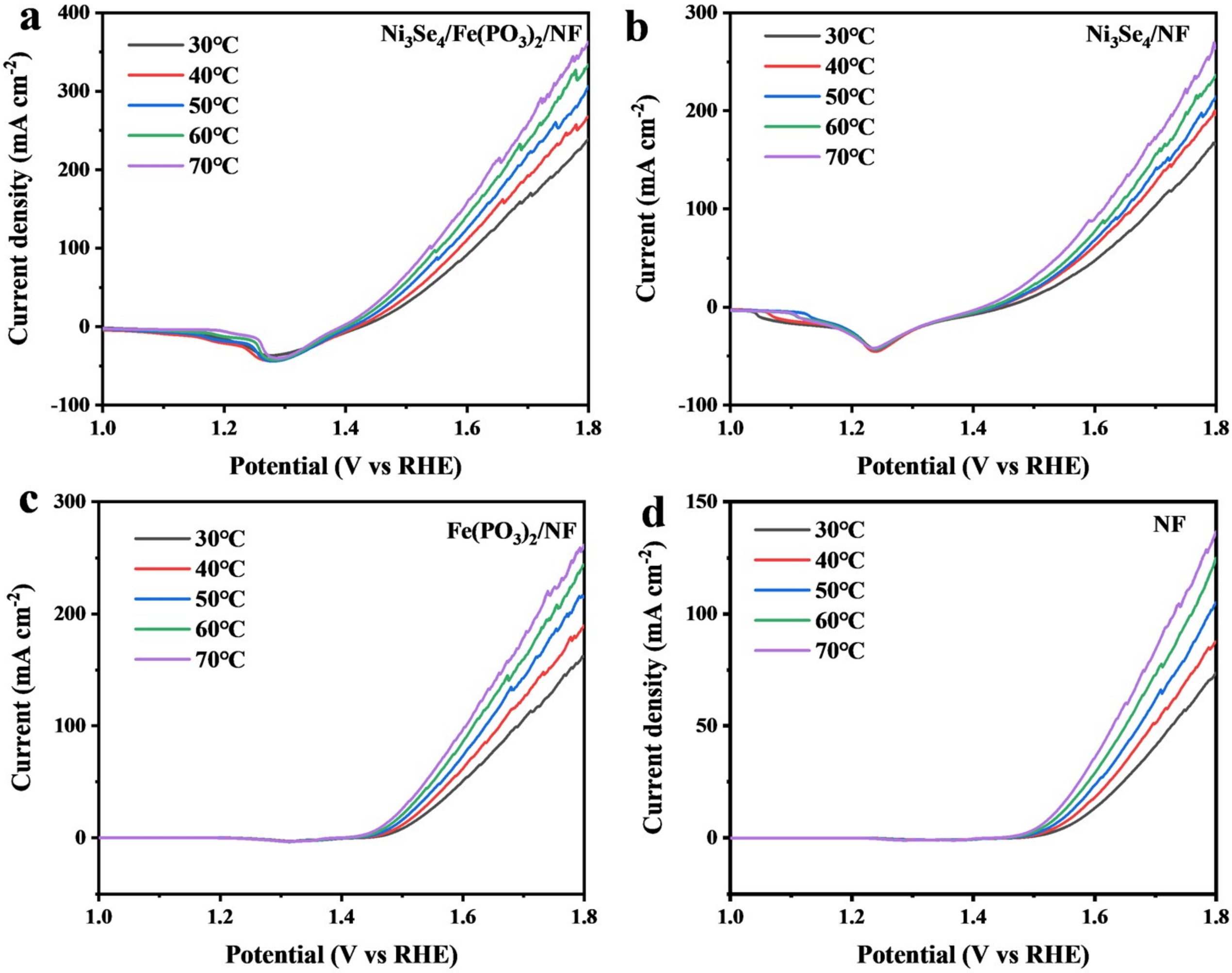

Fig. S2 Polarization curves of (a) $Ni_3Se_4/Fe(PO_3)_2/NF$, (b)Ni_3Se_4/NF, (c) $Fe(PO_3)_2/NF$, (d) NF at different temperatures without IR compensation.

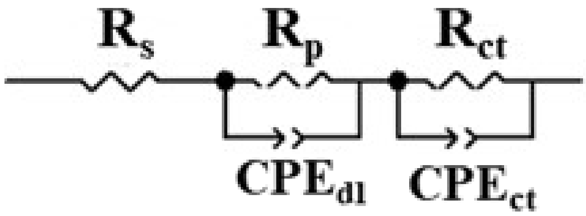

Fig. S3 The equivalent circuit model for electrochemical impedance spectrum fitting.

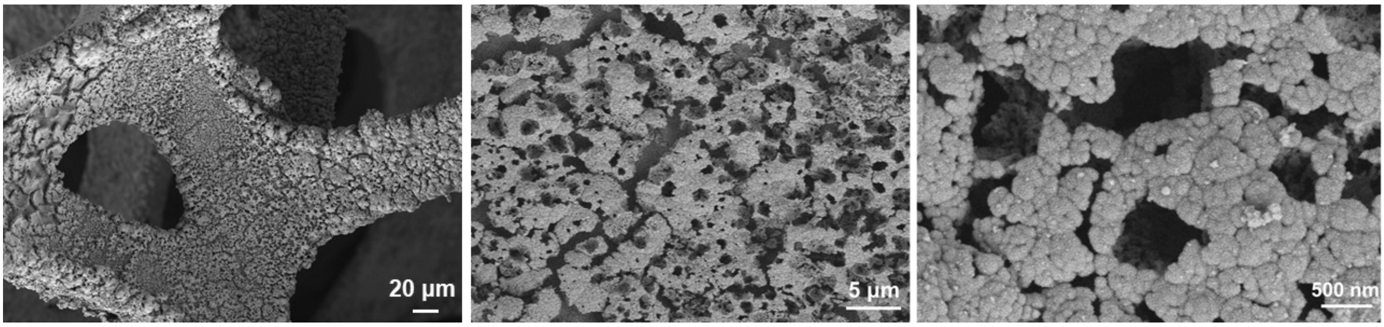

Fig. S4 SEM images of Ni_3Se_4/NF with different magnifications.

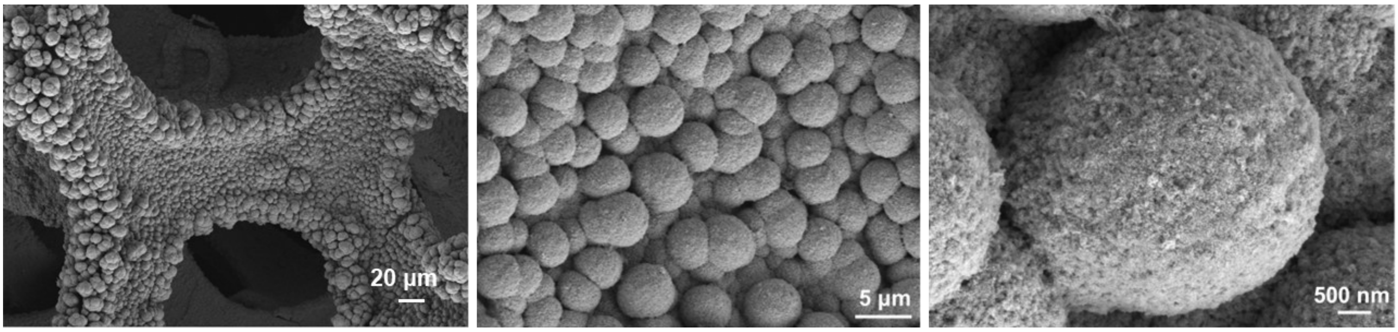

Fig. S5 SEM images of $Fe(PO_3)_3$/NF with different magnifications.

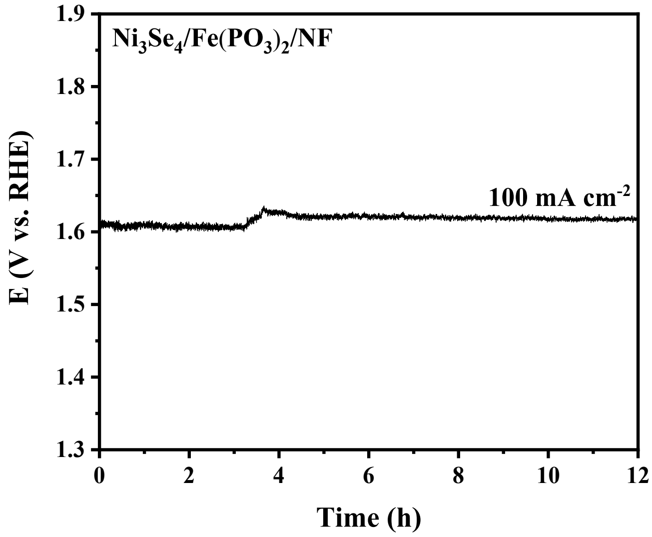

Fig. S6 Stability test of $Ni_3Se_4/Fe(PO_3)_3/NF$ at the current density of 100 mA cm^{-2} for 12 h without IR compensation.

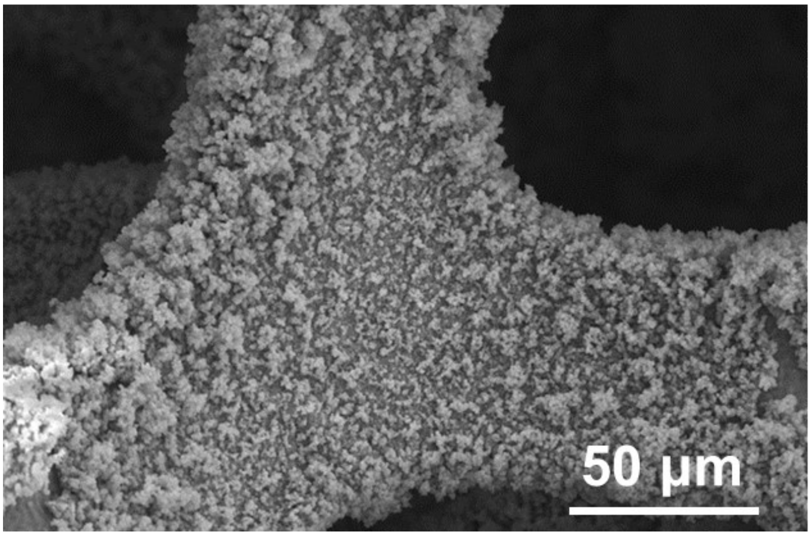

Fig. S7 SEM images of $Ni_3Se_4/Fe(PO_3)_3$/NF after 12 h OER stability test at a constant current density of 10 mA cm^{-2} (the NF skeleton structure was not destroyed).

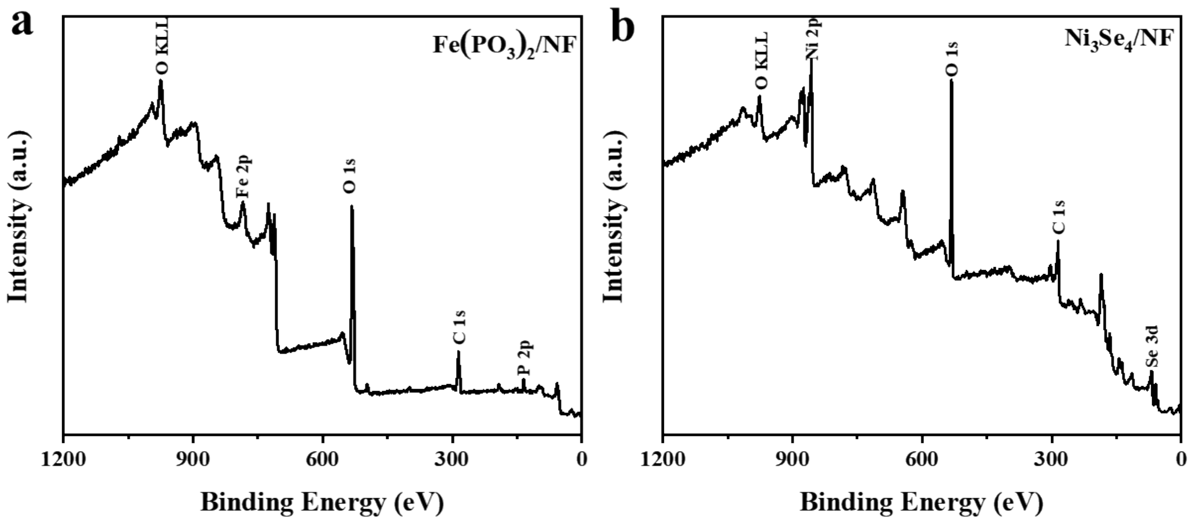

Fig. S8 XPS elemental survey spectra of (a) $Fe(PO_3)_2$/NF and (b) Ni_3Se_4/NF samples.

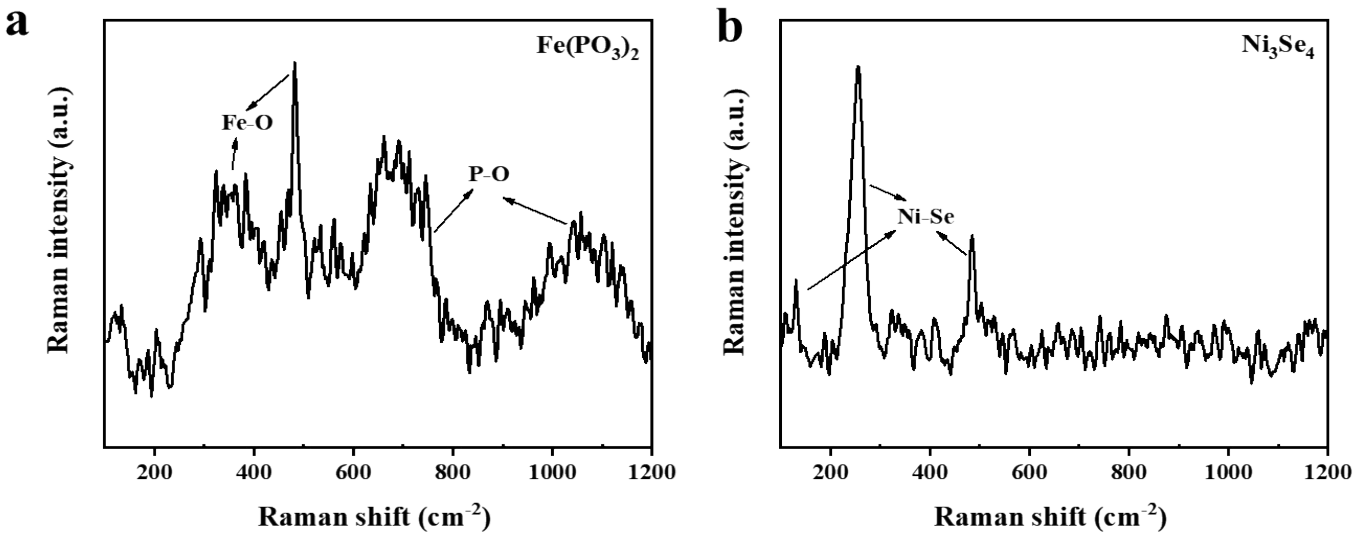

Fig. S9 Raman shift curves of (a) $Fe(PO_3)_2$ and (b) Ni_3Se_4 samples.

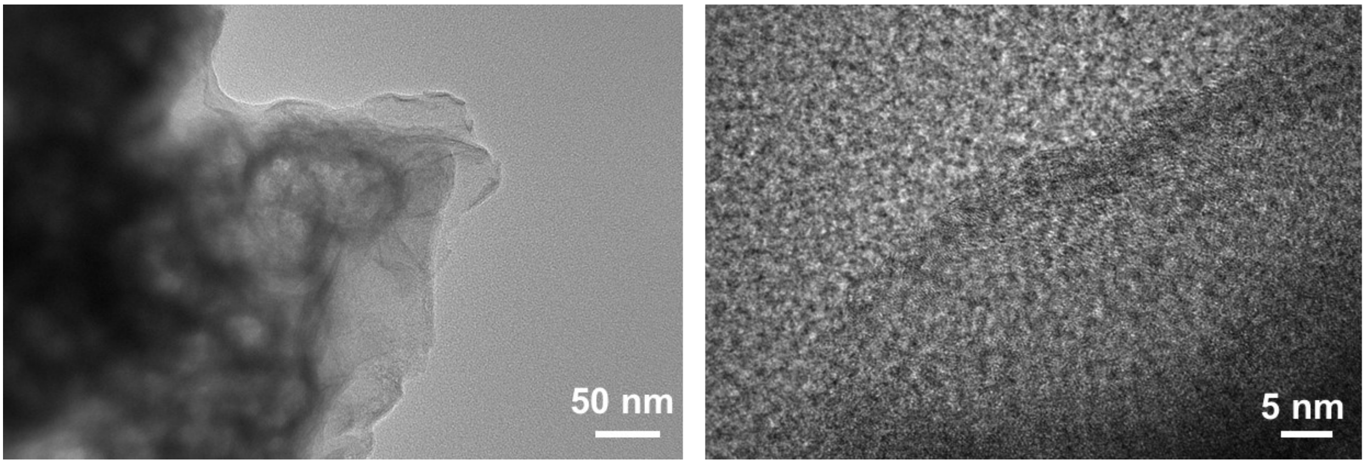

Fig. S10 TEM images of polycrystalline region of $Ni_3Se_4/Fe(PO_3)_2$/NF with different magnifications.

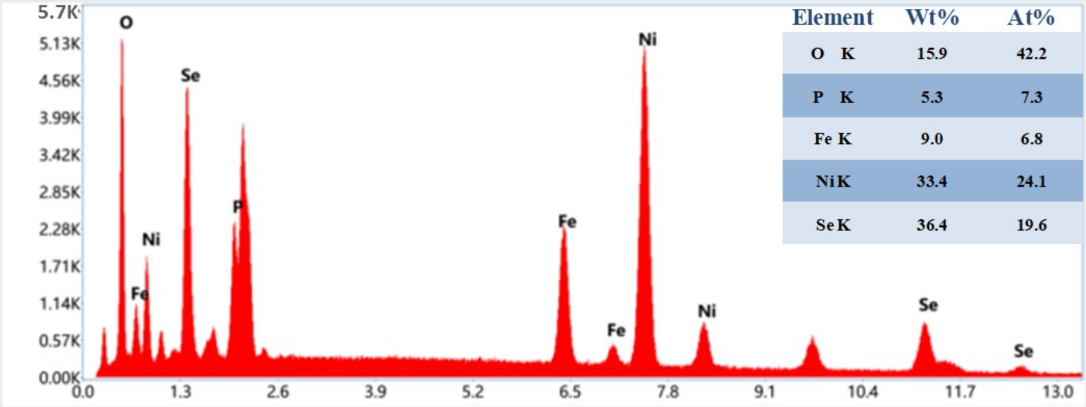

Element	Wt%	At%
O K	15.9	42.2
P K	5.3	7.3
Fe K	9.0	6.8
Ni K	33.4	24.1
Se K	36.4	19.6

Fig. S11 EDS pattern of the $Ni_3Se_4/Fe(PO_3)_2$/NF.

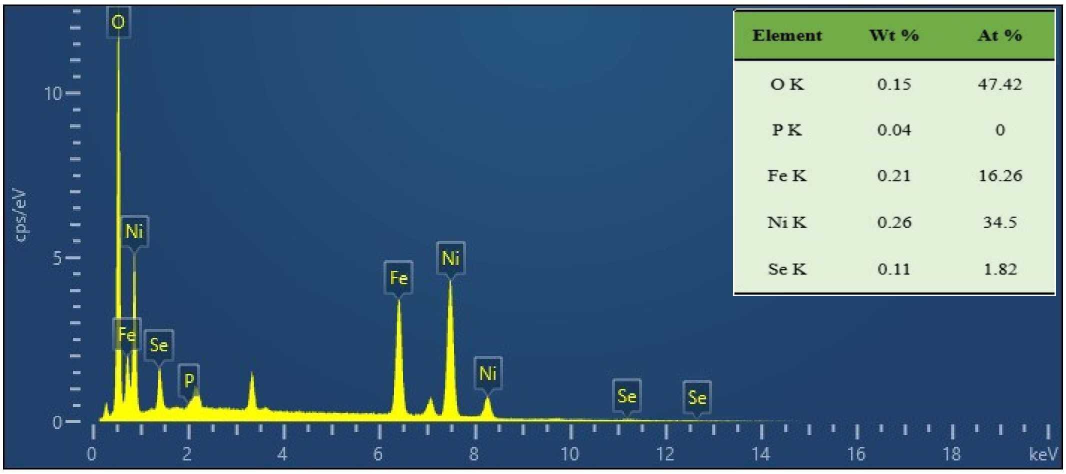

Fig. S12 EDS pattern of the $Ni_3Se_4/Fe(PO_3)_2/NF$ after 12 h stability test at 10 mA cm^{-2}.

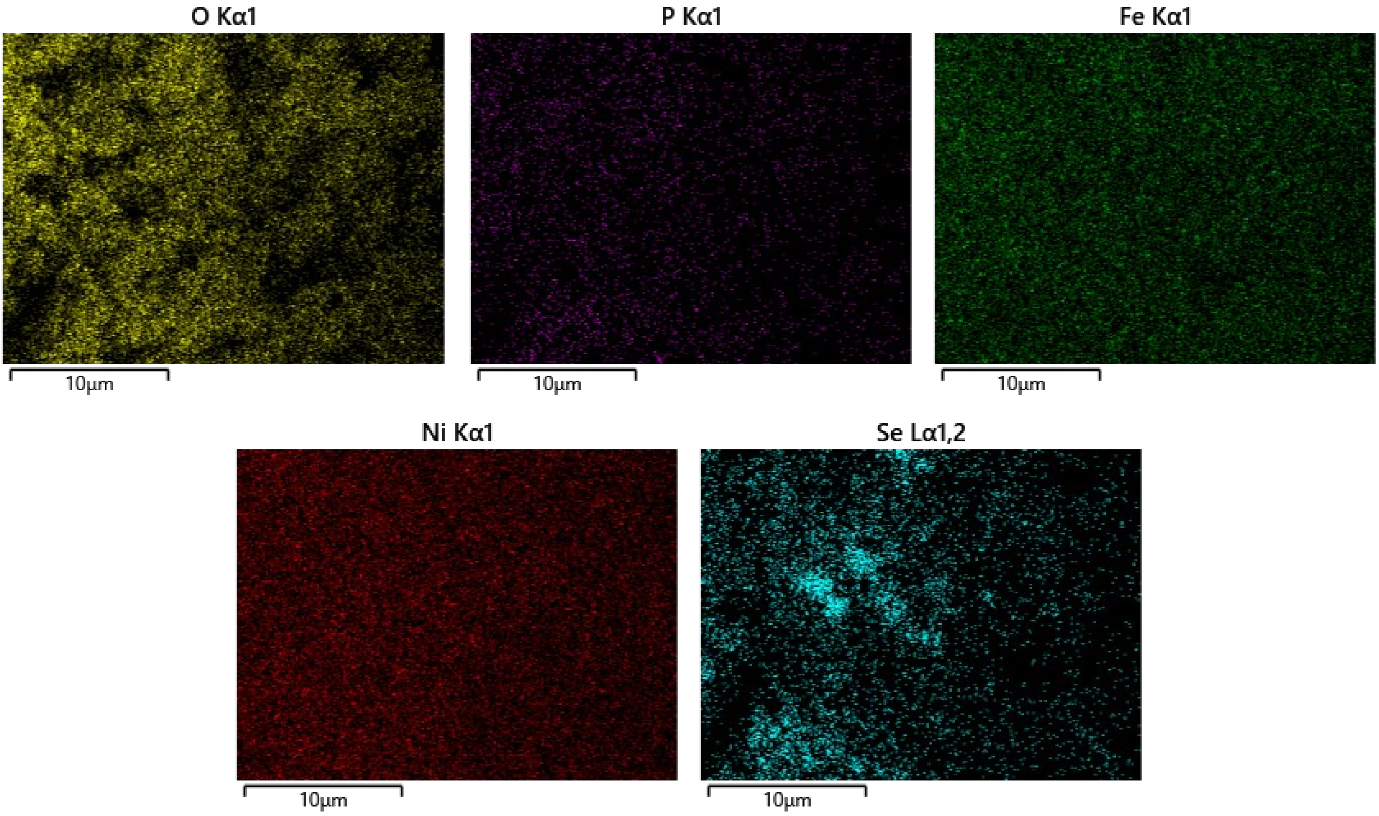

Fig. S13 EDS mappings of Ni, Fe, Se, P in $Ni_3Se_4/Fe(PO_3)_2/NF$ after 12 h stability test at 10 mA cm^{-2}.

Table S1. Summary of EIS fitting results of different catalysts for OER in 1.0 M KOH.

Electrocatalyst	$R_s(\Omega)$	$R_{ct}(\Omega)$	$Rp(\Omega)$
$Ni_3Se_4/Fe(PO_3)_2$/NF	1.408	2.283	0.42865
Ni_3Se_4/NF	1.084	6.602	0.57529
$Fe(PO_3)_2$/NF	1.298	9.664	0.40404
NF	1.318	44.65	1.724

Table S2. BET surface areas, average pore sizes (adsorption) and total pore volumes of various samples.

Sample ID	BET surface area (m^2 g^{-1})	Average pore size (nm)	Pore volume (cm^3 g^{-1})
$Ni_3Se_4/Fe(PO_3)_2$	76.765	3.2506	0.076405
Ni_3Se_4	25.5082	7.5142	0.065105
$Fe(PO_3)_2$	17.312	9.7661	0.052543

Table S3. The mass and molar ratio of Se and P in $Ni_3Se_4/Fe(PO_3)_2$/NF analyzed by ICP-OES.

Element	mass ratio	molar ratio
Se	24.4%	28.4%
P	3.2%	10.4%

Table S4. Summary of Electrochemical double-layer capacitance (C_{dl}) and ECSA of different samples.

Sample	C_{dl} (mF cm^{-2})	ECSA (cm^2)
$Ni_3Se_4/Fe(PO_3)_2/NF$	8.5	212.5
Ni_3Se_4/NF	4.3	107.5
$Fe(PO_3)_2/NF$	2.5	62.5
NF	0.8	20.0

Table S5. Comparisons of the electrocatalytic performance of NiFe-based catalysts for OER in 1.0 M KOH.

Electrocatalyst	Overpotential (mV)	Tafel slope (mV dec^{-1})	Ref
$Ni_3Se_4/Fe(PO_3)_2/NF$	185(η_{10})	30.4	This work
（Ni,Fe）$_3Se_4$	225(η_{10})	41	[1]
Ni_3Se_4/FeOOH	249(η_{10})	46	[2]
Ni_3Se_4/NiFe LDH/CFC	223(η_{10})	55.5	[3]
$Fe(PO_3)_2/Ni_2P/NF$	177(η_{10})	51.9	[4]
CCS-NiFeP-10	201(η_{10})	41.2	[5]
Fe-18h/NF	220(η_{10})	45.2	[6]
Fe-Ni_2P@C/NF	255(η_{200})	64	[7]
Fe-Ni_3S_2	290(η_{100})	46.9	[8]
FeCoNiS/NF	164(η_{10})	23.2	[9]
Fe-Ni_5P_4/NiFeOH-350	221(η_{10})	35.0	[10]
Ni/Fe-MI/OH	229(η_{10})	30.0	[11]
Ni_3S_2/MIL-53(Fe)	214(η_{10})	33.8	[12]
d-NiFe-LDH	230(η_{10})	77.0	[13]
NiFe-LDH/NiS/NF	230(η_{10})	60.1	[14]
Ni_3S_2@Fe-NiP_x/NF	240(η_{100})	46.5	[15]
Fe-NiO/NiS_2	270(η_{10})	40	[16]

References

1 J. Du, Z. Zou, C. Liu and C. Xu, *Nanoscale*, 2018, **10**, 5163-5170.

2 L. Lv, Y. Chang, X. Ao, Z. Li, J. Li, Y. Wu, X. Xue, Y. Cao, G. Hong and C. Wang, *Mater. Today Energy*, 2020, **17**, 100462.

3 T. Zhang, L. Hang, Y. Sun, D. Men, X. Li, L. Wen, X. Lyu and Y. Li, *Nanoscale Horiz.*, 2019, **4**, 1132-1138.

4 H. Zhou, F. Yu, J. Sun, R. He, S. Chen, C. Chu and Z. Ren, *Proc. Natl. Acad. Sci. U. S. A.*, 2017, **114**, 5607-5611.

5 S. Li, L. Wang, H. Su, A. N. Hong, Y. Wang, H. Yang, L. Ge, W. Song, J. Liu, T. Ma, X. Bu and P. Feng, *Adv. Funct. Mater.*, 2022, **32**, 2200733.

6 N. K. Shrestha, S. A. Patil, J. Han, S. Cho, A. I. Inamdar, H. Kim and H. Im, *J. Mater. Chem. A*, 2022, **10**, 8989-9000.

7 D. Li, Z. Li, R. Zou, G. Shi, Y. Huang, W. Yang, W. Yang, C. Liu and X. Peng, *Appl. Catal. B: Environ.*, 2022, **307**, 121170.

8 D. Li, W. Wan, Z. Wang, H. Wu, S. Wu, T. Jiang, G. Cai, C. Jiang and F. Ren, *Adv. Energy Mater.*, 2022, **12**, 2201913.

9 Y. Huang, L. Jiang, H. Liu and J. Wang, *Chem. Eng. J.*, 2022, **441**, 136121.

10 C. Li, J. Zhao, L. Xie, J. Wu and G. Li, *Appl. Catal. B: Environ.*, 2021, **291**, 119987.

11 W. Huang, C. Chen, Z. Ling, J. Li, L. Qu, J. Zhu, W. Yang, M. Wang, K. A. Owusu, L. Qin, L. Zhou and L. Mai, *Chem. Eng. J.*, 2021, **405**, 126959.

12 F. Wu, X. Guo, Q. Wang, S. Lu, J. Wang, Y. Hu, G. Hao, Q. Li, M. Yang and W. Jiang, *J. Mater. Chem. A*, 2020, **8**, 14574-14582.

13 Y. Wu, J. Yang, T. Tu, W. Li, P. Zhang, Y. Zhou, J. Li, J. Li and S. Sun, *Angew. Chem. Int. Edit.*, 2021, **60**, 26829-26836.

14 Q. Wen, K. Yang, D. Huang, G. Cheng, X. Ai, Y. Liu, J. Fang, H. Li, L. Yu and T. Zhai, *Adv. Energy Mater.*, 2021, **11**, 2102353.

15 X. Luo, P. Ji, P. Wang, X. Tan, L. Chen and S. Mu, *Adv. Sci.*, 2022, **9**, 2104846.

16 N. Zhang, Y. Hu, L. An, Q. Li, J. Yin, J. Li, R. Yang, M. Lu, S. Zhang, P. Xi and C. Yan, *Angew. Chem. Int. Edit.*, 2022, **61**, e202207217.